Nuclear Instruments and Methods in Physics Research A 1080 (2025) 170747

Contents lists available at ScienceDirect

Nuclear Inst. and Methods in Physics Research, A

journal homepage: www.elsevier.com/locate/nima

Charge reconstruction from binary hit data on irradiated MALTA2 Czochralski sensors

Lucian Fasselt [a,b,*], Ignacio Asensi Tortajada [c], Prafulla Behera [d], Dumitru Vlad Berlea [a,b], Daniela Bortoletto [e], Craig Buttar [f], Valerio Dao [g], Ganapati Dash [d], Leyre Flores Sanz de Acedo [c], Martin Gazi [e], Laura Gonella [h], Sebastian Haberl [c], Tomohiro Inada [c], Pranati Jana [d], Long Li [i], Heinz Pernegger [c], Petra Riedler [c], Walter Snoeys [c], Carlos Solans Sánchez [c], Milou van Rijnbach [c], Marcos Vázquez Núñez [c], Anusree Vijay [d], Julian Weick [c], Steven Worm [a,b]

[a] Deutsches Elektronen-Synchrotron DESY, Zeuthen, Germany
[b] Humboldt University of Berlin, Berlin, Germany
[c] CERN, Geneva, Switzerland
[d] Indian Institute of Technology Madras, Chennai, India
[e] University of Oxford, Oxford, UK
[f] University of Glasgow, Glasgow, UK
[g] Stony Brook University, New Yorck, United States of America
[h] Università degli Studi di Trieste, Trieste, Italy
[i] University of Birmingham, Birmingham, UK

ARTICLE INFO

Keywords:
DMAPS
180 nm
Tracking
High-energy physics
Charge collection
Irradiation study

ABSTRACT

MALTA2 is a depleted monolithic active pixel sensor (DMAPS) designed for tracking at high rates and is produced in the modified Tower 180 nm CMOS imaging technology. The pixel pitch is 36.4 μm and the sensing layer consists of either high resistivity epitaxial or Czochralski silicon. The implementation of a small collection electrode features a small pixel capacitance and offers low noise. Typically a detection threshold of around 200 e^- is used. It is calibrated making use of a dedicated charge injection circuit on chip and an Fe-55 source. In this contribution, MALTA2 sensors are characterized in terms of hit detection efficiency inside the pixel at fine threshold steps. A comparison is made for samples before and after irradiation at different substrate voltages and with different doping concentration of the internal n-layer. Data was taken at CERN SPS test beam campaigns in 2023 and 2024, using the MALTA beam telescope consisting of six MALTA tracking planes with 4 μm spatial and 2 ns timing resolution. A reconstruction of the most probable signal amplitude from binary hit data is performed. A two-dimensional map of the collected charge is obtained with sub-pixel resolution. The presented method provides an in-beam alternative to grazing angle studies or Edge-TCT for determining a charge collection profile.

1. Introduction

Silicon sensors are crucial for tracking of relativistic charged particles, as they provide excellent detection efficiency while minimizing material budget. Thin detectors with small pixel pitches offer excellent spatial resolution. A promising technology are depleted monolithic active pixel sensors (DMAPS) with a small collection electrode featuring a small pixel capacitance and thus low noise. The property that comes with a small collection electrode is an inhomogeneous electric field inside the depleted silicon. For depositions at the pixel boundaries this leads to increased charge sharing to neighboring pixels and a reduction of collected charge in the seed pixel [1]. The in-pixel charge collection efficiency is not directly measurable for a binary sensor which does not store amplitude information for each hit. This contribution reconstructs the collected charge under the passing of 180 GeV/c charged hadrons from a test beam at CERN SPS acting as minimum ionizing particles (MIPs). The *seed signal*, that is the highest amplitude in a cluster of

* Corresponding author at: Deutsches Elektronen-Synchrotron DESY, Zeuthen, Germany.
E-mail address: lucian.fasselt@desy.de (L. Fasselt).

https://doi.org/10.1016/j.nima.2025.170747
Received 17 April 2025; Received in revised form 4 June 2025; Accepted 6 June 2025
Available online 23 June 2025

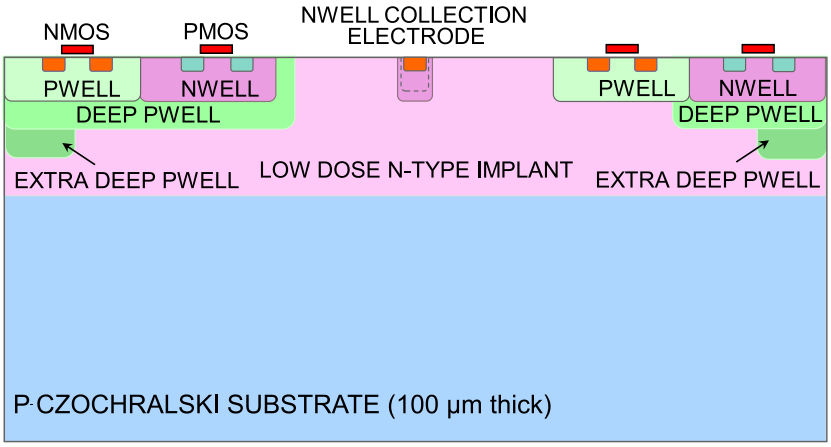

Fig. 1. Cross section of the modified process where an extra deep p-well is added at the edge of the pixel (EDPW) on high resistivity Czochralski substrate. The n^- implant extends the junction for better depletion to the full pixel pitch of 36.4 µm. The diameter of the hexagonal collection electrode is 2 µm. The image is not drawn to scale.

pixels, is reconstructed and described through the most probable value (MPV) of the Landau-distribution. A beam telescope tracks particles with a resolution well below the pixel pitch and makes it possible to reconstruct the MPV at an in-pixel level. Additionally, the depth in silicon is estimated which is equivalent to the reconstructed charge and here called *visible depth*. An important aspect in the development of tracking detectors is the study of radiation hardness. The *visible depth* is a quantity to characterize the signal formation after irradiation and can be used as a benchmark for simulation studies. The performance of neutron irradiated sensors up to a fluence of 5×10^{15} 1 MeV n_{eq}/cm^2 is compared for different doping modifications.

2. Methods

2.1. MALTA2 sensor

MALTA2 is a DMAPS designed for radiation-hard future tracking applications at high rates > 100 MHz/cm^2. It is produced in the modified Tower Semiconductor 180 nm CMOS imaging technology. The readout is binary and asynchronous to minimize data rate and power consumption [2]. The sensing layer of the 36.4×36.4 µm^2 pixels consists of either high resistivity epitaxial (EPI) or Czochralski (CZ) silicon with a resistivity of 3–4 kΩ cm [3]. The small octagonal n^+ collection electrode with 2 µm diameter is located at the pixel center (Fig. 1). All measurements presented here are performed with MALTA2 samples on 100 µm thick CZ silicon with two different doping levels of the low dose n-type implant. This n-layer generates a more uniform depletion of the sensor and separates the deep p-well of the pixel circuit from the p-type substrate. The doping levels compared here are denoted high (H-dop) and very high (VH-dop), where the latter has an approximately 70 % increased implantation dose [4]. A MALTA2 sensor consists of 224 × 512 pixels and covers the area of 8×19 mm^2. The front-end design enables a low detection threshold. For an optimized detection efficiency above 99 %, a threshold is typically set within the range of 200 to 400 e^- [5]. The threshold smearing due to pixel-to-pixel variations is before irradiation of the order of 10% and the uncertainty on the mean threshold 3%. For this study, the sensors are configured in a low gain setting by reducing the front-end bias current. This increases the threshold to values > 400 e^- and enables the sensitivity to the charge deposition of a MIP by measuring a decrease in efficiency at high thresholds.

2.2. MALTA telescope

The MALTA2 sensors are mounted as a device under test (DUT) in the MALTA beam telescope and irradiated samples are cooled to −20 °C to avoid annealing and suppress noise. The MALTA beam telescope is permanently installed at the H6 beamline at the Super Proton Synchrotron (SPS) at CERN providing access to the charged hadron beam of 180 GeV/c. The beam telescope consists of six MALTA sensors for triggering and track reconstruction as well as a scintillator for precise timing reference. Up to two DUTs can be mounted and characterized. Tracks are reconstructed at the location of the DUT with a spatial resolution of 4.1 ± 0.2 µm and a track timing resolution of 2.1 ns [6]. The precise spatial resolution offers the possibility to resolve the efficiency with in-pixel resolution. A detection efficiency is obtained by matching hits in the DUT with the reconstructed tracks from the telescope.

2.3. Threshold scan

Tracking sensors are usually designed to operate at low threshold offering large hit detection efficiency. As for MALTA2, the readout is often only binary without any amplitude information for data rate reduction. By changing the threshold in fine steps, the amplitude of the collected charge can be reconstructed [7]. For each threshold the tracking efficiency is determined and shown in Fig. 2 for tracks reconstructed to pass close to the pixel center with an average radial distance of $\Delta R = 1.6$ µm. The threshold dependent efficiency data (triangles) is sensitive to the integral of the collected charge distribution. The energy loss of a MIP traversing silicon can be approximated by the Landau probability density function (pdf). Its complementary cumulative distribution function (ccdf) is the upper tail integral and is applied as a fit function to the data and is defined by

$$\mathrm{ccdf}(x) = \int_x^{+\infty} p(x')dx' \tag{1}$$

where the Landau distribution is expressed in the form

$$p(\lambda) = \frac{1}{2\pi i}\int_{c-i\infty}^{c+i\infty} e^{\lambda s + s\ln(s)} ds. \tag{2}$$

The maximum of $p(\lambda)$ is defined as the MPV and corresponds to the position of the inflection point of $\mathrm{ccdf}(x)$. It serves as the quantity for charge reconstruction and is determined for each in-pixel position.

3. Results

3.1. Charge reconstruction from binary hit data

The 2 × 2 pixel matrix of Fig. 3 sorts the MPVs into 2.3×2.3 µm^2 bins based on their associated track position within the pixel. While the deposited charge is independent of the in-pixel location, the collected charge is reduced by charge sharing. At the pixel center, the two

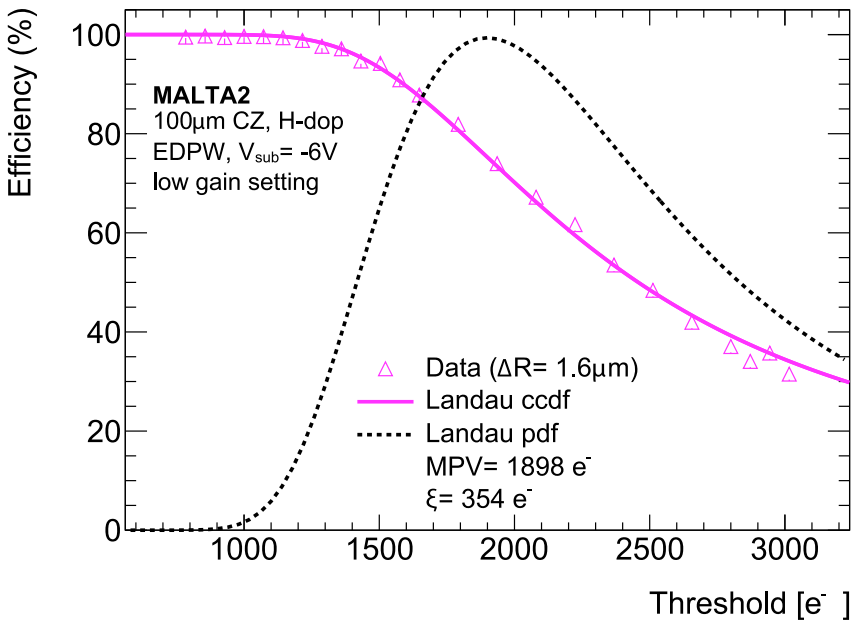

Fig. 2. Efficiency distribution at the pixel center versus threshold. A fit of the upper tail integral of the Landau distribution is performed through which its most probable value (MPV) and width are extracted. The corresponding Landau pdf is shown for illustration (dashed line).

quantities are equal because all deposited charge is assumed to be collected at a single electrode as one hit clusters. The charge values range from roughly 1900 e^- at the pixel center to 1550 e^- at the pixel corner. The dominant uncertainty is that on the mean threshold of 3%. Equal charge sharing on the boundary of two pixels is expected to reduce the seed signal to 50 %. This region is found to be thin compared to the tracking uncertainty of 4.1 µm leading to a higher convoluted charge at the boundaries.

3.2. Visible depth

Experimentally, the most probable energy loss through ionization of a MIP is parameterized in [8] for thin silicon thicknesses of 5.6 µm < x < 120 µm as

$$\Delta_p\,[\mathrm{keV}] = x(0.126 + 0.027\ln x). \tag{3}$$

For a given value of the MPV and the electron–hole pair creation energy of 3.66 eV the formula can be inverted to obtain the corresponding depth in silicon, here called visible depth. It is added as an additional z-axis to Fig. 3. The calculation assumes ideal charge collection where all deposited charge inside the depleted region is collected by a single pixel. These assumptions are met close to the pixel center where at a substrate voltage of −6 V a depth of 32 µm is found. For an increased substrate voltage of −7 V the substrate is further depleted and the central depth increases to 38 µm. For comparison, MALTA2 sensors on 30 µm epitaxial silicon are fully depleted at −6 V which has been validated by the reconstruction of a 30 µm visible depth as well as Edge-Transient Current Technique (E-TCT) [9]. Consequently, Czochralski sensors detect a larger charge amplitude due to deeper depletion than a 30 µm EPI sensor.

4. Irradiation comparison

MALTA2 sensors have been neutron irradiated at different fluences up to 5×10^{15} 1 MeV n_{eq}/cm^2 of non-ionizing energy loss (NIEL) at the Triga reactor in the Institute Jožef Stefan (IJS), Slovenia. Earlier studies have already characterized MALTA2 samples with very high doping of the n-layer after irradiation to 3×10^{15} 1 MeV n_{eq}/cm^2 which exceeds the expected lifetime fluence for the outer layers of the inner pixel detectors of ATLAS and CMS at the High Luminosity LHC [10,11]. With an average cluster size of 1.7 pixels an efficiency above > 97 % is determined [4].

4.1. Substrate voltage increase

The relevant radiation damage mechanisms are donor removal in the low dose n-type implant and an increase in the effective p-type doping of the substrate [3]. The substrate resistivity decreases and thus one effective measure is to increase the substrate voltage to further deplete the sensor. This clearly improves the average efficiency over the whole sensor, as seen in Fig. 4. Consequently the MPV increases due to better depletion of the substrate. At the pixel center, the visible depth increases from 15 to 26 to 30 µm for the voltages -10, −20 and −30 V, respectively.

4.2. Doping increase of n-implant

The efficiency performance of various sensors is compared in Fig. 5(a) after irradiation. Hit clusters in the DUT are matched with the extrapolated telescope tracks only if they lie within a radius of 80 µm [6]. For the efficiency determination the number of matched tracks is divided by all reconstructed tracks. The noise level of the DUTs is below 40 Hz per pixel [4]. This ensures that noise does not contribute to the efficiency determination. Generally, sensors irradiated with larger fluences yield a smaller efficiency at the same threshold: At a threshold of 1000 e^-, the efficiency at the pixel center is > 99 % before irradiation and decreases to around 96 %, 77 % and 50 % for the H-dop samples irradiated to 1, 2 and 3×10^{15} 1 MeV n_{eq}/cm^2. This generally leads to a decrease in reconstructed charge in terms of MPV. At the irradiation fluences of 3 and 5×10^{15} 1 MeV n_{eq}/cm^2, sensors with increased doping of the low dose n-type implant (VH-dop) are compared to the sensors with lower doping (H-dop) and are up to 20 % more efficient at the same threshold. They can withstand the donor removal longer until the benefit of the low dose n-type implant disappears. This is also reflected in the reconstructed visible depth (Fig. 5(b)). For the lowest irradiation fluence the substrate voltage increase is still sufficient to recover the depth of a non irradiated senor of 30 µm. However higher fluences lead to a reduced visible depth that cannot be recovered solely by a voltage increase. For each sensor the depth at maximum substrate voltage are compared in Fig. 6. The depth is doubled from 5 to 10 µm for the highest irradiated samples simply due to the doping increase of the n-layer. In the future, sensors with even higher doping are to be tested. However, the benefit in depletion

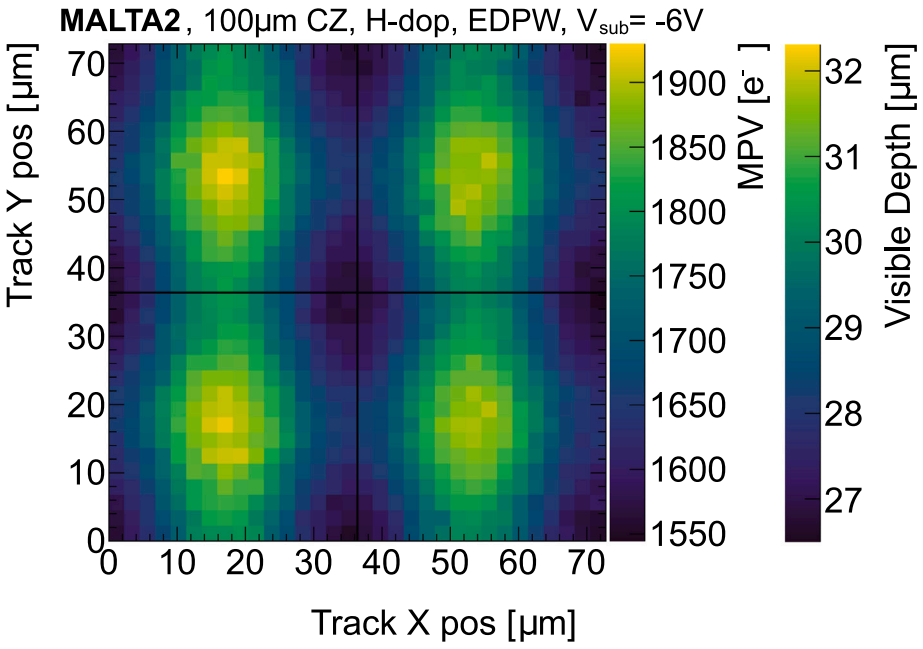

Fig. 3. Most probable value of the energy loss (MPV) projected onto a 2 × 2 pixel matrix. The MPVs are sorted into $2.3 \times 2.3\,\mu m^2$ bins based on their associated track position within the pixel extracted from the telescope data. The decrease in charge at the pixel boundaries is due to charge sharing. The second z-axis shows the corresponding depth in silicon.

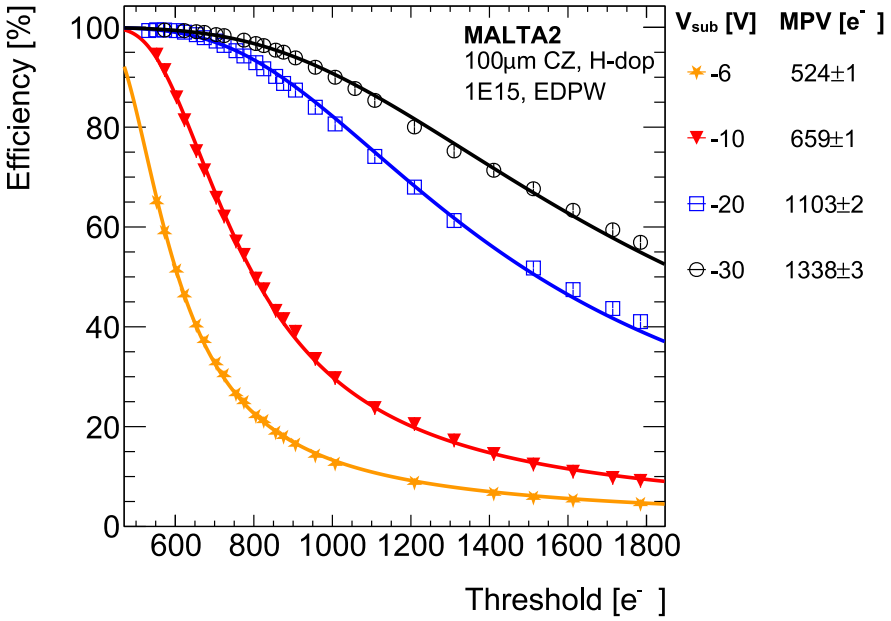

Fig. 4. Average efficiency versus threshold for different substrate bias voltage. The sensor has been irradiated to 1×10^{15} 1 MeV n_{eq}/cm^2. Larger reverse bias recovers the efficiency due to better depletion of the substrate.

is expected to come with the cost of larger pixel capacitance and noise because once the n^- doping approaches that of the n^+ collection electrode, the design cannot be considered that of a small electrode anymore.

5. Conclusion

The hit efficiency of various MALTA2 sensors is determined with the MALTA telescope at SPS at fine threshold steps. The charge in terms of the most probable value (MPV) is reconstructed through a Landau fit and quantifies the corresponding visible depth in silicon for different in-pixel positions. At the pixel center, depths up to 38 µm are determined. After irradiation the efficiency at the same threshold degrades which causes the MPV and visible depth to reduce. Performance after irradiation is partly recovered by

- Increase in substrate voltage.
- Increased doping of continuous n-layer.

In the future, sensors with even higher doping are to be tested for potentially more radiation hardness under the sacrifice of higher noise. The presented method recovers amplitude information on a statistical basis despite the purely binary hit information. It is viable to obtain

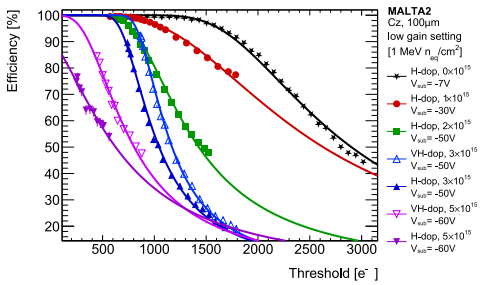

(a) Efficiency distribution at the pixel center.

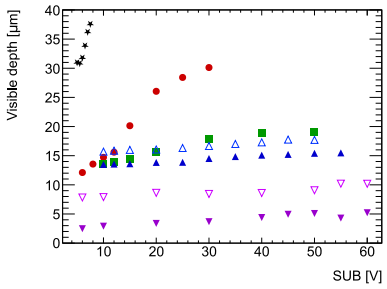

(b) Visible depth at the pixel center versus substrate voltage

Fig. 5. Irradiation comparison. (a) shows the efficiency at the pixel center for different irradiation fluences and highest substrate voltage. The visible depth in silicon at the pixel center (b) generally increases with substrate voltage. For fluences at 3 and 5×10^{15} 1 MeV n_{eq}/cm^2 (blue and purple markers) two sensors are compared. The ones with increased doping (VH-dop, hollow markers) show improved efficiency and increased visible depth. The effect of doping is larger than the substrate voltage increase.

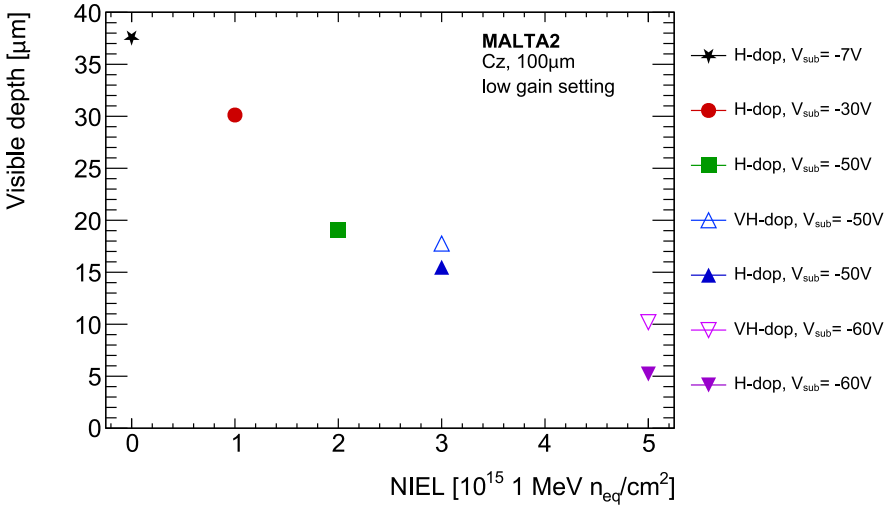

Fig. 6. Maximum visible depth at the pixel center versus irradiation fluence in terms of non-ionizing energy loss (NIEL). With increasing fluence, the reconstructed charge and thus the visible depth decreases. Samples with very high doping of the n-type implant (VH-dop, hollow markers) degrade less than samples with high doping (H-dop) due to a prolonged doping lifetime after irradiation.

a two dimensional charge collection profile in terms of MPV. Other techniques such as the Transient Current Technique have the advantage of directly measuring the amplitude but are restricted to edge illumination of individual analog pixels. A two dimensional top view is usually not accessible due to metal layers that absorb the laser light. Alternatively, grazing angle studies give a direct tool to quantify the average depletion depth of a pixel but are not sensitive to in-pixel resolution and instead provide one depth estimate for the whole sensor. The method presented here is based on threshold scans paired with the tracking capabilities of a beam telescope and provide a statistical tool for amplitude reconstruction with sub-pixel resolution. It will help in the future to select doping modifications and simulate them for improved radiation hardness.

Declaration of competing interest

The authors declare that they have no known competing financial interests or personal relationships that could have appeared to influence the work reported in this paper.

Acknowledgment

This project has received funding from the European Union's Horizon 2020 Research and Innovation programme under Grant Agreement numbers 101004761 (AIDAinnova), 675587 (STREAM), and 654168 (IJS, Ljubljana, Slovenia).

References

[1] M. Munker, et al., Simulations of CMOS pixel sensors with a small collection electrode, improved for a faster charge collection and increased radiation tolerance, J. Instrum. 14 (05) (2019) C05013, http://dx.doi.org/10.1088/1748-0221/14/05/C05013.

[2] R. Cardella, et al., MALTA: an asynchronous readout CMOS monolithic pixel detector for the ATLAS high-luminosity upgrade, J. Instrum. 14 (06) (2019) C06019, http://dx.doi.org/10.1088/1748-0221/14/06/C06019.

[3] H. Pernegger, et al., MALTA-Cz: a radiation hard full-size monolithic CMOS sensor with small electrodes on high-resistivity Czochralski substrate, J. Instrum. 18 (09) (2023) P09018, http://dx.doi.org/10.1088/1748-0221/18/09/P09018.

[4] Milou van Rijnbach, et al., Radiation hardness of MALTA2 monolithic CMOS imaging sensors on Czochralski substrates, Eur. Phys. J. C 84 (3) (2024) 251, http://dx.doi.org/10.1140/epjc/s10052-024-12601-3, arXiv:2308.13231.

[5] Lucian Fasselt, et al., Charge calibration of MALTA2, a radiation hard depleted monolithic active pixel sensor, 2025, arXiv:2501.13562.

[6] Milou van Rijnbach, et al., Performance of the MALTA telescope, Eur. Phys. J. C 83 (7) (2023) 581, http://dx.doi.org/10.1140/epjc/s10052-023-11760-z, arXiv:2304.01104.

[7] David-Leon Pohl, et al., Obtaining spectroscopic information with the ATLAS FE-I4 pixel readout chip, Nucl. Instrum. Methods A 788 (2015) 49–53, http://dx.doi.org/10.1016/j.nima.2015.03.067.

[8] S. Meroli, et al., Energy loss measurement for charged particles in very thin silicon layers, J. Instrum. 6 (06) (2011) P06013, http://dx.doi.org/10.1088/1748-0221/6/06/P06013.

[9] D.V. Berlea, et al., Depletion depth studies with the MALTA2 sensor, a depleted monolithic active pixel sensor, Nucl. Instrum. Methods A 1063 (2024) 169262, http://dx.doi.org/10.1016/j.nima.2024.169262.

[10] ATLAS Collaboration, Technical Design Report for the ATLAS Inner Tracker Strip Detector, Tech. Rep., CERN, Geneva, 2017.

[11] E. Migliore, CMS pixel detector design for HL-LHC, J. Instrum. 11 (12) (2016) C12061, http://dx.doi.org/10.1088/1748-0221/11/12/C12061.